

On the Downlink Coverage Performance of RIS-Assisted THz Networks

Waqas Aman, *Member, IEEE*, Nour Kouzayha, *Member, IEEE*, Muhammad Mahboob Ur Rahman, *Member, IEEE*, and Tareq Y. Al-Naffouri, *Senior Member, IEEE*

Abstract—This letter provides a stochastic geometry (SG)-based coverage probability (CP) analysis of an indoor terahertz (THz) downlink assisted by a single reconfigurable intelligent surface (RIS) panel. Specifically, multiple access points (AP) deployed on the ceiling of a hall (each equipped with multiple antennas) need to serve multiple user equipment (UE) nodes. Due to presence of blockages, a typical UE may either get served via a direct link, the RIS, or both links (the composite link). The locations of the APs and blockages are modelled as a Poisson point process (PPP) and SG framework is utilized to compute the CP, at a reference UE for all the three scenarios. Monte-Carlo simulation results validate our theoretical analysis.

I. INTRODUCTION

Reconfigurable intelligent surfaces (RIS) which turn the hostile wireless propagation from foe to a friend, and the previously unused but enormous terahertz (THz) band (from 0.3-10 THz) are now appreciated as two key enablers for upcoming 6G cellular standard [1]. Stochastic geometry (SG), on the other hand, is a theoretical tool that provides the average coverage performance of a communication system with a random/ad-hoc node geometry to gain useful system-level insights (e.g., impact of various important system parameters on the overall coverage probability) [2]. SG has been utilized to study the performance of a wide range of different wireless network configurations [3].

Contributions. This letter is the first study on the average coverage performance of an indoor RIS-assisted THz downlink with multiple APs, multiple UEs and a single RIS panel (amid multiple blockages). The main contribution of this work is as follows. For a typical UE, we compute the CP, i.e., signal-to-interference ratio (SIR) being greater than a threshold, for the three distinct scenarios, i.e., when only the direct link is available, when only the RIS link is available, and when both links (aka composite link) are available. The analytical results are validated by means of Monte-Carlo simulations.

Related work. There exist quite a few works that do SG-based coverage probability (CP) analysis of RIS-assisted wireless communication networks. Authors in [4] compute the CP of a RIS-assisted downlink where a fraction of the user equipment (UE) nodes is considered direct users, while the remaining UEs are served by the RIS. [5] computes the CP of a RIS-assisted system where the locations of both the access points (AP) and RIS panels are modeled as a Gauss point process in the 2D space. [6] utilizes the SIR to compute the CP for a RIS-assisted millimeter (mm)-wave communication system. Authors in [7] consider multiple RIS panels at random locations to compute the CP in a mm-wave cellular network.

The authors are with King Abdullah University of Science and Technology (KAUST), Saudi Arabia. Emails: {waqas.aman, nour.kouzayha, muhammad.rahman, tareq.alnaffouri}@kaust.edu.sa.

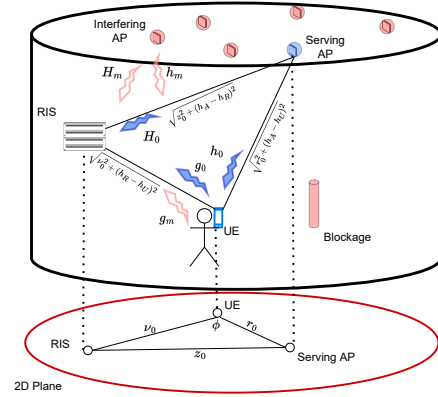


Fig. 1: System Model

Finally, the authors in [8] compute the CP to quantify the benefit of RIS panels in the presence of random (humans and buildings) blockages, in a mm-wave cellular network.

II. SYSTEM MODEL

Network Model: We consider a finite indoor THz network consisting of multiple APs deployed on the ceiling at a fixed height h_A and a single RIS panel to serve users in the downlink as shown in Fig. 1. We consider the performance of a reference user (UE) located at the origin $\mathbf{o} = (0, 0, 0)$ with a single antenna of gain G_U and at a fixed height h_U from the ground level. The locations of the APs are abstracted by a homogeneous Poisson point process (PPP) $\Pi_A = \{x_i\}$ of intensity λ_A , where x_i denotes the 2D location of the i -th AP. The finite region $D = b(\mathbf{o}', R_t)$ is modeled as a disk of radius R_t centered around $\mathbf{o}' = (0, 0, h_A - h_U)$. Each AP is equipped with N_A antennas and transmits with power P_A . We assume that the RIS panel is attached to a wall at fixed height h_R and horizontal distance v_0 from the UE and has a total of $N = N_x \times N_y$ elements, where N_x and N_y are the numbers of RIS elements along the x-axis and y-axis, respectively. Finally, we assume an interference-limited scenario, and thus, ignore additive noise in our analysis and focus on the signal-to-interference-ratio (SIR) only to get the coverage probability. **Blockage Model:** We consider random blockages (humans, objects) modeled as cylinders of radius r_B and height h_B where the midpoints of cylinders are modeled as a PPP Π_B with intensity λ_B . Thus, the link between the AP and the UE located at a 2D distance r can be blocked and the AP-UE line-of-sight (LoS) probability is given as

$$P_{\text{LoS}}^{\text{LoS}}(r) = \exp(-\beta_D r), \quad (1)$$

where $\beta_D = 2\lambda_B r_B |\frac{h_B - h_U}{h_A - h_U}|$. The probability that the AP-UE link is blocked is the non-line-of-sight (NLoS) probability given as

$P_D^{\text{NLoS}}(r) = 1 - P_D^{\text{LoS}}(r)$. Similarly, the the RIS-UE link can be blocked and the RIS-UE LoS probability is given as

$$P_R^{\text{LoS}} = \exp(-\beta_R v_0), \quad (2)$$

where $\beta_R = 2\lambda_B r_B |\frac{h_B - h_U}{h_R - h_U}|$. $P_R^{\text{NLoS}} = 1 - P_R^{\text{LoS}}$ is the probability that the RIS-UE link is blocked. Finally we assume that the links between then RIS and the APs are always in a LoS condition as the RIS is higher than existing blockages. The set of non-blocked APs with direct links to the UE Π_A can be obtained by thinning the PPP of APs with the LoS probability $P_D^{\text{LoS}}(r)$ and is therefore a non-homogeneous PPP with intensity $\lambda_D(r) = \lambda_A P_D^{\text{LoS}}(r)$.

Association Policy: The reference UE associates with the nearest AP to get service. We define a direct link as the link between the UE and the nearest AP. The RIS link denotes the indirect link to the nearest AP through the RIS panel. Due to the presence of random blockages, there are three ways a UE could get served: i) the direct link is available but the RIS link is blocked, ii) the RIS link is available but the direct link is blocked, iii) both links are available (we call such link a composite link). In all three cases, the UE receives (either direct or through-RIS) interference from the other APs.

III. PRELIMINARIES: RECEIVED SIGNAL ANALYSIS

We write down the expressions for the pathloss, received signal, received signal power, and interference power for the direct link, RIS link, and composite link below.

A. Direct Link

Pathloss Model: The pathloss for the direct link between the UE and an AP located at a 2D distance r is given as [9]:

$$PL_D(r) = \frac{G_U G_A c^2}{(4\pi f)^2} e^{-k_a(f)\sqrt{r^2 + (h_A - h_U)^2}} (r^2 + (h_A - h_U)^2)^{-1}, \quad (3)$$

where G_A , G_U are the transmit and receive antenna's gain respectively, f is the operating frequency, c is the speed of light, $k_a(f)$ is the absorption coefficient, and $\sqrt{r^2 + (h_A - h_U)^2}$ is the 3D distance between the AP and the associated UE.

Received Signal Power: When the direct line-of-sight (LoS) link is available, the received signal at the typical UE from its serving AP at a 2D distance of r_0 is given by: $y_D = \sqrt{P_A PL_D(r_0)} \mathbf{h}_0^T \mathbf{f}_0 x$, where P_A is the AP transmit power, x is the transmitted symbol, $\mathbf{h}_0 = [h_1, \dots, h_{N_A}]^T$ is the channel vector and $h_j \sim \mathcal{CN}(0, 1)$ is the channel gain between the UE and the j -th antenna of the AP, and $\mathbf{f}_0 = [f_1, \dots, f_{N_A}]^T$ is the precoding vector. Then, the received signal power becomes

$$S_D = P_A PL_D(r_0) |\mathbf{h}_0^T \mathbf{f}_0 x|^2. \quad (4)$$

Interference: The interference seen by the UE on the direct link can be expressed as

$$I_D = P_A \frac{G_U G_A c^2}{(4\pi f)^2} \sum_{m \in \Pi_D / 0} \frac{e^{-k_a(f)\sqrt{r_m^2 + (h_A - h_U)^2}}}{(r_m^2 + (h_A - h_U)^2)} |\mathbf{h}_m^T \mathbf{f}_m x|^2, \quad (5)$$

where Π_D denotes the non-homogeneous PPP (of intensity λ_D) of all the APs with direct links.

B. RIS Link

Pathloss: The pathloss of the AP-RIS-UE link is given as

$$PL_R(z) = \frac{G_U G_A (L_x L_y)^2}{(4\pi)^2 (z^2 + (h_A - h_R)^2) (v_0^2 + (h_R - h_U)^2)} \times e^{-k_a(f)\sqrt{z^2 + (h_A - h_R)^2}} e^{-k_a(f)\sqrt{v_0^2 + (h_R - h_U)^2}} F(\theta), \quad (6)$$

where z is the 2D distance between the AP and the RIS, L_x and L_y are the length and width of a RIS element, $F(\theta) = \cos^2(\theta) = \frac{(h_A - h_R)^2}{z^2 + (h_A - h_R)^2}$, θ is the incident angle of the AP, $\sqrt{z^2 + (h_A - h_R)^2}$ is the distance between the AP and the RIS, and $\sqrt{v_0^2 + (h_R - h_U)^2}$ is the RIS-UE distance.

Received Signal Power: The received signal through the RIS link from the serving AP located at a 2D distance r_0 from the UE can be expressed as $y_R = \sqrt{P_A PL_R(z_0)} \mathbf{g}_0^T \mathbf{\Phi} \mathbf{H}_0 \mathbf{f}_0 x$, where $z_0 = \sqrt{r_0^2 + v_0^2} - 2r_0 v_0 \cos \phi$ is the 2D distance separating the RIS from the serving AP, $PL_R(\cdot)$ is the total pathloss, $\mathbf{H}_0 \in \mathbb{C}^{N \times N_A}$ is the channel matrix between serving AP and RIS, $\mathbf{g}_0 \in \mathbb{C}^{N \times 1}$ is the RIS-UE channel vector and $\mathbf{\Phi} \in \mathbb{C}^{N \times N}$ is a diagonal matrix defined as: $\mathbf{\Phi} = \text{diag}(\text{vect}[\hat{\mathbf{\Phi}}])$ where $\text{vect}[\mathbf{A}]$ vectorizes the matrix \mathbf{A} , $\hat{\mathbf{\Phi}} \in \mathbb{C}^{N_x \times N_y}$ and $[\hat{\mathbf{\Phi}}]_{m,n} = e^{j\varphi_{m,n}}$, where $\varphi_{m,n}$ is the phase shift of the (m, n) RIS element [10]. Then, the received signal power is given as

$$S_R = P_A PL_R(z_0) |\mathbf{g}_0^T \mathbf{\Phi} \mathbf{H}_0 \mathbf{f}_0 x|^2, \quad (7)$$

Interference: The interference on the RIS link is given as

$$I_R = \Omega \sum_{m \in \Pi_A / 0} \frac{e^{-k_a(f)\sqrt{z_m^2 + (h_A - h_R)^2}}}{(z_m^2 + (h_A - h_R)^2)} F(\theta_m) |\mathbf{g}_m^T \mathbf{\Phi} \mathbf{H}_m \mathbf{f}_m x|^2, \quad (8)$$

where $\Omega = P_A \frac{G_U G_A (L_x L_y)^2 e^{-k_a(f)\sqrt{v_0^2 + (h_R - h_U)^2}}}{(4\pi)^2 (v_0^2 + (h_R - h_U)^2)}$, z_m is the 2D distance separating the m -th AP from the RIS, and $F(\theta_m) = \cos^2(\theta_m)$, where θ_m is the incident angle for the m -th AP.

C. Composite Link

The net received signal on the composite link is the sum of the two signals received due to the two individual but parallel links (i.e., a direct link and RIS link)

$$y_C = y_D + y_R = \sqrt{P_A} \left(\sqrt{PL_D(r_0)} \mathbf{h}_0^T + \sqrt{PL_R(z_0)} \mathbf{g}_0^T \mathbf{\Phi} \mathbf{H}_0 \right) \mathbf{f}_0 x. \quad (9)$$

Thus, the net received signal power of the composite link can be expressed as

$$S_C = P_A |(\sqrt{PL_D(r_0)} \mathbf{h}_0^T + \sqrt{PL_R(z_0)} \mathbf{g}_0^T \mathbf{\Phi} \mathbf{H}_0) \mathbf{f}_0 x|^2. \quad (10)$$

Finally, the interference on the composite link can be expressed as $I_C = I_D + I_R$.

IV. COVERAGE ANALYSIS

In this section, we derive the association probability through direct, RIS, and composite links in addition to the conditional and overall coverage probabilities.

A. User Association Probability

The UE can connect to the nearest AP through a direct non blocked link or through the RIS if the direct link is blocked. The UE can also use both links as a composite link if both are not blocked. The association probabilities for the three scenarios are given in the following lemma whose proof

follows from the definition of the association scenarios and the LoS and NLoS probabilities given in (1) and (2).

Lemma 1: Conditioned on the distance r_0 between the UE and the nearest AP, the association probabilities through direct, RIS and composite links, denoted as $A_D(r_0)$, $A_R(r_0)$ and $A_C(r_0)$, respectively, are given as

$$A_D(r_0) = \exp(-\beta_D r_0) (1 - \exp(-\beta_R v_0)). \quad (11)$$

$$A_R(r_0) = (1 - \exp(-\beta_D r_0)) \exp(-\beta_R v_0). \quad (12)$$

$$A_C(r_0) = \exp(-\beta_D r_0) \exp(-\beta_R v_0). \quad (13)$$

B. Statistics of Received Signal Power and Interference

In this section, we provide the distribution of the received signal power and Laplace transform of interference in the three coverage scenarios.

Lemma 2: The desired signal power through the RIS \mathcal{S}_R given in (7) follows the exponential distribution with parameter $\kappa_R(z_0) = (2N^2(P_{APL_R}(z_0) \sum_{j=1}^{N_A} |f_j|^2))^2$.

Proof: In this work, we set the design/control parameter Φ as $\Phi = \text{diag}[\frac{g}{\|g\|}]$. Thus, the received signal through the RIS link can be expressed as

$$\begin{aligned} \mathcal{S}_R &= P_{APL_R}(z_0) |\mathbf{1}^T \mathbf{H}_0 \mathbf{f}_0 x|^2 = P_{APL_R}(z_0) \left| \sum_{j=1}^{N_A} f_j \sum_{i=1}^N h_{i,j} \right|^2 \\ &= P_{APL_R}(z_0) |f_1(h_{11} + h_{21} + \dots + h_{N1}) + f_2(h_{12} + h_{22} + \dots + h_{N2}) \\ &\quad \dots + f_{N_A}(h_{1N_A} + h_{2N_A} + \dots + h_{NN_A})|^2. \end{aligned} \quad (14)$$

By rearranging the summation terms inside the absolute square as $(f_1 h_{11} + f_2 h_{12} + \dots + f_{N_A} h_{1N_A}) + (f_1 h_{N1} + f_2 h_{N2} + \dots + f_{N_A} h_{NN_A})$ and letting $Z_i = (f_1 h_{i1} + f_2 h_{i2} + \dots + f_{N_A} h_{iN_A})$, the dual-summation term in (14) can be written as $\sum_{j=1}^{N_A} f_j \sum_{i=1}^N h_{i,j} = \sum_{i=1}^N Z_i$, where $Z_i \sim \mathcal{CN}(0, \sum_{j=1}^{N_A} |f_j|^2)$. The summation in (14) is equivalent to a summation of N i.i.d. random variables and follows the $\mathcal{CN}(0, N \sum_{j=1}^{N_A} |f_j|^2)$ distribution. Finally, the term $|\mathbf{g}^H \Phi \mathbf{H}_0 \mathbf{f}_0|$ is Rayleigh distributed with parameter $N \sum_{j=1}^{N_A} |f_j|^2$ and \mathcal{S}_R is exponentially distributed with parameter $\kappa_R(z_0) = \frac{1}{2N^2(P_{APL_R}(z_0) \sum_{j=1}^{N_A} |f_j|^2)^2}$. ■

The distribution of the desired signal power through the composite link \mathcal{S}_C is given in the following lemma whose proof follows a similar procedure as in Lemma 2.

Lemma 3: The desired signal power through the composite link \mathcal{S}_C given in (10) follows the exponential distribution with parameter $\kappa_C(r_0, z_0) = \frac{1}{(\sqrt{2}(NPL_R(z_0) + PL_D(r_0)) \sum_{j=1}^{N_A} |f_j|^2)^2}$.

Next, we derive the Laplace transform of interference from direct APs I_D , through the RIS I_R and through composite links I_C in the following Lemmas.

Lemma 4: Conditioning on the 2D distance r_0 between the UE and the serving AP, the Laplace transform of the aggregate interference from all APs with direct links with respect to the reference UE is given as

$$\mathcal{L}_{I_D}(s) = \exp \left[-2\pi\lambda_A \int_{r_0}^{R_t} \left(1 - \frac{\kappa_D}{\kappa_D + sP_{APL_D}(r)} \right) P_{D^{\text{LoS}}}(r) r dr \right], \quad (15)$$

where $\kappa_D = \frac{1}{2(\sum_{j=1}^{N_A} |f_j|^2)^2}$, $P_{D^{\text{LoS}}}(\cdot)$ is LoS probability given in (1), and $PL_D(\cdot)$ is the pathloss of the direct link given in (3).

$$\begin{aligned} \text{Proof:} \quad &\text{The Laplace transform } \mathcal{L}_{I_D}(s) \text{ can be derived as} \\ &\mathcal{L}_{I_D}(s) = \mathbb{E}_{I_D} [e^{-sI_D}] \stackrel{(a)}{=} \mathbb{E}_{\Pi_D, \gamma_m} \left[\exp \left(-s \sum_{m \in \Pi_D / 0} P_{APL_D}(r_m) \gamma_m \right) \right] \\ &\stackrel{(b)}{=} \mathbb{E}_{\Pi_D} \left[\prod_{m \in \Pi_D / 0} \frac{\kappa_D}{\kappa_D + sP_{APL_D}(r_m)} \right], \end{aligned} \quad (16)$$

where (a) is obtained by defining $\gamma_m = |\mathbf{f}_m \mathbf{h}_m|^2$, and (b) is obtained from the distribution of γ_m which follows the exponential distribution with parameter $\kappa_D = \frac{1}{2(\sum_{j=1}^{N_A} |f_j|^2)^2}$. The expression in (15) is finally obtained by omitting the index m and after applying the probability generating functional (PGFL) on the PPP of direct APs with intensity $\lambda_A P_{D^{\text{LoS}}}(r)$. ■

Lemma 5: Conditioning on the 2D distance r_0 between the UE and the serving AP, the Laplace transform of the aggregate interference from all APs having non-blocked links through the RIS with respect to the reference UE is given as

$$\begin{aligned} \mathcal{L}_{I_R}(s) &= \exp \left[-2\pi\lambda_A \int_0^\pi \int_{r_0}^{R_t} \left(1 - Q \left(sP_{APL_R} \left(\sqrt{r^2 + v_0^2 - 2rv_0 \cos \phi} \right) \right) \right) r dr d\phi \right], \end{aligned} \quad (17)$$

where $Q(x) = \frac{1}{\sqrt{1+2x}} \exp \left(-\frac{\kappa_I x}{1+2x} \right)$, $\kappa_I = \frac{\mu_B}{2(\sum_{j=1}^{N_A} |f_j^m|) \sigma_B^2}$, $\mu_B = \frac{\pi}{2}$, $\sigma_B^2 = 2^2 \left(1 - \frac{\pi^2}{16} \right)$, $PL_R(\cdot)$ is the pathloss of the direct link given in (6) and v_0 is the 2D RIS-UE distance.

Proof: First, we derive the distribution of the term $\zeta_m = |\mathbf{g}_m^T \Phi \mathbf{H}_m \mathbf{f}_m|^2 = |\sum_{j=1}^{N_A} f_j^m \sum_{i=1}^N g_i^m h_{i,j}^m e^{-\iota\psi_i}|^2$ in the interference through RIS link expression in (8). Using the polar form of the complex numbers and by letting $B_{i,j}^m = |g_i^m||h_{i,j}^m|$, and $\tau_{i,j}^m = \theta_{g_i^m} + \theta_{h_{i,j}^m} - \psi_i$, we can write the summation as

$$\begin{aligned} &\sum_{j=1}^{N_A} |f_j^m| e^{\iota\theta_{f_j^m}} \sum_{i=1}^N |g_i^m||h_{i,j}^m| e^{\iota(\theta_{g_i^m} + \theta_{h_{i,j}^m} - \psi_i)} \\ &= \sum_{j=1}^{N_A} |f_j^m| e^{\iota\theta_{f_j^m}} \sum_{i=1}^N B_{i,j}^m e^{\iota\tau_{i,j}^m} \stackrel{(a)}{\leq} \sum_{i=1}^N B_i^m \sum_{j=1}^{N_A} |f_j^m|, \end{aligned} \quad (18)$$

where (a) is obtained by replacing $B_{i,j}$ with B_i since $B_{i,j}^m \forall i, j$ are i.i.d. Note that $B_{i,j}^m$ is the product of two independent Rayleigh distributed random variables and has a mean $\mu_B = \frac{\pi}{2}$, and variance $\sigma_B^2 = 2^2 \left(1 - \frac{\pi^2}{16} \right)$. The expression in (18) can be expressed as $\sum_{i=1}^N C_{N_A} B_i$, where $C_{N_A} = \sum_{j=1}^{N_A} |f_j^m|$. As N is significantly large in a typical RIS panel, we can invoke the central limit theorem (CLT) and $\sum_{i=1}^N C_{N_A} B_i$ will follow a normal distribution with mean $N C_{N_A} \mu_B$ and variance $N C_{N_A}^2 \sigma_B^2$. Consequently, $|\mathbf{g}_m^T \Phi \mathbf{H}_m \mathbf{f}_m x|^2$ follows a non-central chi-squared distribution $\chi_1^2(\kappa_I)$ with one degree of freedom and non-centrality parameter $\kappa_I = \frac{1}{2} \frac{\mu_B}{C_{N_A} \sigma_B^2}$.

The Laplace transform of RIS interference is derived as

$$\begin{aligned} \mathcal{L}_{I_R}(s) &= \mathbb{E}_{I_R} \left[\exp \left(-s \Omega \sum_{m \in \Pi_A / 0} \frac{e^{-k_a(f) \sqrt{z_m^2 + (h_A - h_R)^2}} (h_A - h_R)^2}{(z_m^2 + (h_A - h_R)^2)^2} \zeta_m \right) \right] \\ &\stackrel{(a)}{=} \mathbb{E}_{\Pi_A} \left[\prod_{m \in \Pi_A / 0} Q \left(s \Omega \frac{e^{-k_a(f) \sqrt{z_m^2 + (h_A - h_R)^2}} (h_A - h_R)^2}{(z_m^2 + (h_A - h_R)^2)^2} \right) \right], \end{aligned} \quad (19)$$

where (a) is obtained from the independence of $\zeta_m = |\mathbf{g}_m^T \Phi \mathbf{H}_m \mathbf{f}_m|^2$ and Π_A and from the moment generating

function (MGF) $Q(x)$ of ζ_m which follows the non-central Chi-square distribution, i.e., $Q(x) = \frac{1}{\sqrt{1+2x}} \exp\left(-\frac{\kappa_1 x}{1+2x}\right)$. The final expression of $\mathcal{L}_{I_R}(s)$ given in (17) is obtained by applying the PGFL on the APs PPP Π_A and by reformulating z_m using the cosine rule as a function of the angle and 2D distance from UE to m -th AP, i.e. $z_m = \sqrt{r_m^2 + v_0^2 - 2r_m v_0 \cos \phi_m}$. ■

Corollary 1: The Laplace transform of interference from composite links includes the interference from direct links and RIS links and is given as $\mathcal{L}_{I_C}(s) = \mathcal{L}_{I_D}(s)\mathcal{L}_{I_R}(s)$, where $\mathcal{L}_{I_D}(s)$ and $\mathcal{L}_{I_R}(s)$ are given in (15) and (17), respectively.

C. Coverage Probability

Since the UE has three different coverage scenarios, the overall coverage probability is derived using the law of total probability and is given in the following theorem.

Theorem 1: The coverage probability of the reference UE in a RIS-assisted downlink THz network is given as

$$P_{\text{Cov}} = \int_0^\pi \frac{1}{\pi} \int_0^{R_t} f_{r_0}(r_0) (A_D(r_0)P_D(r_0) + A_R(r_0)P_R(r_0, \phi_0) + A_C(r_0)P_C(r_0, \phi_0)) dr_0 d\phi_0, \quad (20)$$

where $f_{r_0}(r_0)$ is the PDF of the 2D distance separating the UE from the nearest AP and is given as $f_{r_0}(r_0) = 2\pi\lambda_A r_0 \exp(-\lambda_A \pi r_0^2)$, $A_D(r_0)$, $A_R(r_0)$ and $A_C(r_0)$ are given in Lemma 1 and $P_D(r_0)$, $P_R(r_0)$ and $P_C(r_0)$ are the conditional coverage probabilities given the three coverage scenarios and are expressed as

$$P_D(r_0) = \mathcal{L}_{I_D}\left(\frac{\tau\kappa_D}{P_A \text{PL}_D(r_0)}\right), \quad (21)$$

$$P_R(r_0, \phi_0) = \mathcal{L}_{I_D}(\tau\kappa_R(z_0)) \mathcal{L}_{I_R}(\tau\kappa_R(z_0)), \quad (22)$$

$$P_C(r_0, \phi_0) = \mathcal{L}_{I_D}(\tau\kappa_C(r_0, z_0)) \mathcal{L}_{I_R}(\tau\kappa_C(r_0, z_0)), \quad (23)$$

where $z_0 = \sqrt{r_0^2 + v_0^2 - 2r_0 v_0 \cos \phi_0}$, $\mathcal{L}_{I_D}(\cdot)$ and $\mathcal{L}_{I_R}(\cdot)$ are the Laplace transform of interference through the direct and the RIS links and are given in (15) and (17), respectively.

Proof: The conditional coverage probability for a direct link $P_D(r_0)$ is defined as the SIR on the direct link is higher than a predefined threshold τ and can be derived as

$$P_D(r_0) = \mathbb{P}\left[\frac{\mathcal{S}_D}{I_D} > \tau\right] = \mathbb{P}\left[|\mathbf{h}_0^T \mathbf{f}_0|^2 > \frac{\tau I_D}{P_A \text{PL}_D(r_0)}\right] \stackrel{(a)}{=} \mathbb{E}_{I_D}\left[\exp\left(-\kappa_D \tau \frac{I_D}{P_A \text{PL}_D(r_0)}\right)\right] \stackrel{(b)}{=} \mathcal{L}_{I_D}\left(\frac{\tau\kappa_D}{P_A \text{PL}_D(r_0)}\right), \quad (24)$$

where (a) follows from the complementary cumulative distribution function (CCDF) of the channel and antenna gain parameter $|\mathbf{h}_0^T \mathbf{f}_0|^2$ which follows the exponential distribution with parameter $\kappa_D = \frac{1}{2(\sum_{i=1}^{N_A} |f_i|^2)^2}$ and (b) follows from the definition of the Laplace transform of the interference from APs with direct links I_D .

When, the RIS link is not blocked, the UE can receive interference from all APs through the RIS and from APs with non-blocked direct links. Thus, the conditional coverage probability for a RIS link can be derived as

$$P_R(r_0, \phi_0) = \mathbb{P}\left[\frac{\mathcal{S}_R}{I_R + I_D} > \tau\right] \stackrel{(a)}{=} \mathbb{E}\left[\exp(-\tau\kappa_R(z_0)(I_R + I_D))\right], \quad (25)$$

where (a) is obtained from the exponential distribution of the received signal power \mathcal{S}_R derived in Lemma 2. The final

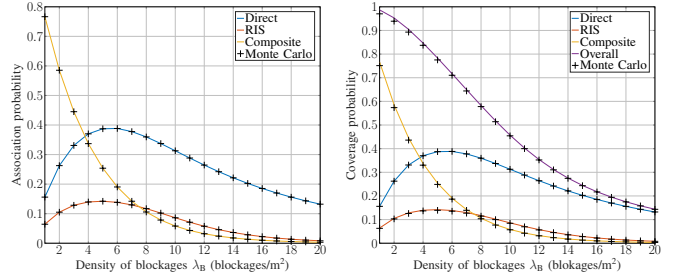


Fig. 2: Association probabilities as function of λ_B .

expression in (22) is obtained using the definition of Laplace transform and the independence of direct and RIS interference I_D and I_R when conditioned on the 2D distance and angle to nearest AP r_0 and ϕ_0 . The conditional coverage probability for the composite link is obtained following the same procedure and the final expression is given in (23). Finally, the overall coverage probability can be obtained by using the total law of probability and deconditionning with respect to r_0 and ϕ_0 which has a uniform distribution in $[0, \pi]$. ■

V. NUMERICAL RESULTS

In this section, we validate the analytical results by conducting intensive Monte-Carlo simulations for an RIS-assisted indoor THz downlink network. Unless otherwise stated, we set $P_A = 1$ mW, $N_A = 10$ antennas, $f = 0.3$ THz, $k_a(f) = 0.075$ m $^{-1}$, $L_x = L_y = \frac{c}{2f}$, $R_t = \sqrt{140}$ m, $h_A = 3$ m, $h_U = 1$ m, $h_R = 0.75 h_A$, $v_0 = \sqrt{2}$ m, $r_B = 0.22$ m, $h_B = 1.63$ m (height of a human), $\lambda_B = 2$ blockages/m 2 , $G_A = G_U = 30$ dB, and $N = 10^7$ RIS elements. We assume that every antenna is transmitting with unit energy i.e., $|f_j|^2 = 1$, $\forall j$. The Monte-Carlo simulations are conducted for 10^6 realizations of the homogeneous PPP of APs and for h_j , g_i , $[\mathbf{H}]_{i,j} \sim \mathcal{CN}(0, 1)$, $\forall i \in \{1..N\}$, $j \in \{1..N_A\}$.

Fig. 2 and Fig. 3 present the analytical (solid lines) and Monte-Carlo simulations (markers) results of the association and coverage probabilities as a function of the intensity of blockages λ_B . Fig. 2 and Fig. 3 show a close match between the simulations and analytical results which validates the analysis developed in Section IV. As the density of blockages increases, the direct-only and RIS-only association probabilities start to increase then decrease gradually while association through composite links is always decreasing with λ_B . This is because a lower number of blockages provides a high chance of availability of both links (composite). However, with the existence of more blockages, the composite link association probability drops below the direct and RIS-only cases. As the RIS is deployed at a lower height than the APs, the RIS link is more likely to be blocked than the direct link. Thus, the direct association probability outperforms association through RIS. On the other hand, the overall coverage probability drops with the increase of λ_B as more APs with good channel conditions will be blocked. Such behavior is different than the direct only case where the coverage probability shows an optimal λ_B at which the coverage probability is maximized.

Fig. 4 shows the impact of the RIS height and distance with respect to the typical UE. We can clearly note that moving the RIS away from UE decreases the coverage probability due

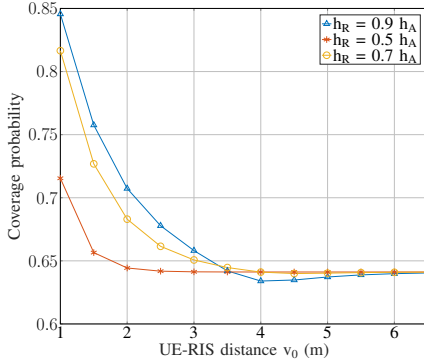


Fig. 4: Coverage probability as function of the UE-RIS distance and the RIS height.

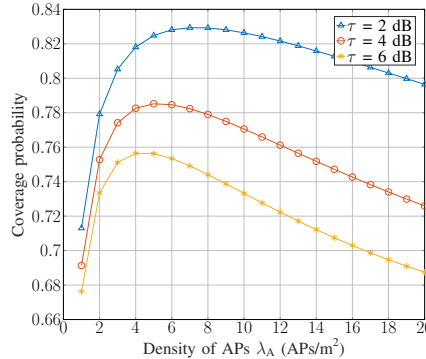


Fig. 5: Coverage probability as function of the density of APs and SIR threshold.

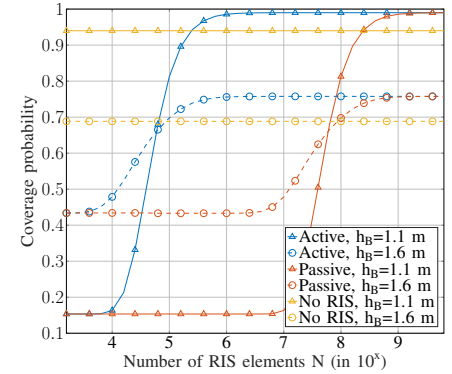


Fig. 6: Coverage probability as function of RIS elements and blockages height.

to the increased pathloss. At a certain UE-RIS distance, the coverage probability stabilizes as the UE sticks to the connection through the direct link and the RIS has no contribution on the coverage performance. Fig. 4 also shows that moving the RIS closer to APs provides better coverage probability for low UE-RIS distances. A higher RIS height increases the LoS probability of the RIS link and improves as result the composite link coverage probability since an alternative link exists with higher probability when the direct link is blocked.

Fig. 5 highlights the impact of the density of APs on the overall coverage probability for different SIR thresholds. A higher density of APs increases the chance of having a nearby non-blocked AP to serve the UE, thus improving the coverage probability. This happens up to some extent after which increasing further the density of APs causes a degradation in the coverage probability due to the increased level of interference on both direct and RIS links. Thus, an optimal density of APs should be deployed to maximize the coverage probability. The optimal density of APs is larger for low SIR thresholds which show an improved performance compared to high SIR threshold values.

Finally, Fig. 6 presents the coverage probability as a function of the number of RIS elements N and the height of blockages and compare an RIS-assisted THz network with a passive RIS, an active RIS and the case of a THz network when no RISs are implemented. The active RIS is implemented by considering an extra gain $G_R = 30$ dB provided by the existing RIS. As the number of RIS elements increases, the coverage probability increases till a certain point after which adding more RIS elements does not affect the overall coverage probability. The reason behind this saturation is that the association probabilities are not functions of N , while the conditional coverage probabilities reach their maximum value of 1. For a low number of RIS elements, a higher blockage height increases the coverage probability for the active and passive RIS cases. However, when N increases, a higher blockages height negatively affects the coverage probability. This is due to the fact that the composite link is significantly dominant for the blockages with lower height, while the direct link is dominant for the blockages with more heights.

Fig. 6 also shows that an active RIS starts providing coverage gains when the number of RIS elements exceeds $10^{5.3}$ for $h_B = 1.1$ m and 10^5 for $h_B = 1.6$ m. On the other side, a passive RIS requires relatively larger numbers of RIS

elements ($10^{8.5}$ for $h_B = 1.1$ m and 10^8 for $h_B = 1.6$ m) to overcome the impact of increased pathloss and molecular absorption losses at THz frequencies. We note here that, although THz frequencies allow for adding more RIS elements with reasonable panel sizes, a large RIS panel is required to provide reasonable gains in THz networks. Furthermore, optimal RIS placement is required to mitigate the impact of blockages and increased losses at high frequencies.

VI. CONCLUSION

We investigated a RIS-assisted THz network with blockages. Using SG tool, we derived tractable expressions for the coverage probability for three different coverage scenarios: Direct-only, RIS-only and composite. Monte-Carlo simulations were conducted to validate the analytical outcomes of the letter. The obtained results highlight the importance of optimizing RIS deployment to extend the coverage of THz networks amid interference and blockages, and identify clear trade-offs in terms of RIS panel sizes and energy consumption.

REFERENCES

- [1] Z. Zhang, Y. Xiao, Z. Ma, M. Xiao, Z. Ding, X. Lei, G. K. Karagiannidis, and P. Fan, “6g wireless networks: Vision, requirements, architecture, and key technologies,” *IEEE Vehicular Technology Magazine*, vol. 14, no. 3, pp. 28–41, 2019.
- [2] M. Haenggi, *Stochastic geometry for wireless networks*. Cambridge University Press, 2012.
- [3] Y. Hmamouche, M. Benjillali, S. Saoudi, H. Yanikomeroglu, and M. D. Renzo, “New trends in stochastic geometry for wireless networks: A tutorial and survey,” *Proceedings of the IEEE*, vol. 109, no. 7, pp. 1200–1252, 2021.
- [4] T. Shafique, H. Tabassum, and E. Hossain, “Stochastic geometry analysis of irs-assisted downlink cellular networks,” *IEEE Trans. on Commun.*, vol. 70, no. 2, pp. 1442–1456, 2022.
- [5] T. Wang, G. Chen, M.-A. Badiu, and J. P. Coon, “Performance analysis of RIS-assisted large-scale wireless networks using stochastic geometry,” *arXiv preprint arXiv:2208.08773*, 2022.
- [6] M. Nemati, J. Park, and J. Choi, “Ris-assisted coverage enhancement in millimeter-wave cellular networks,” *IEEE Access*, vol. 8, pp. 188 171–188 185, 2020.
- [7] X. Shi, N. Deng, N. Zhao, and D. Niyato, “Coverage enhancement in millimeter-wave cellular networks via distributed IRSs,” *IEEE Trans. on Commun.*, 2022.
- [8] Z. Li, H. Hu, J. Zhang, and J. Zhang, “Ris-assisted mmwave networks with random blockages: Fewer large RISs or more small RISs?” *IEEE Trans. on Wireless Commun.*, 2022.
- [9] N. Kouzayha, M. A. Kishk, H. Sarieddeen, M.-S. Alouini, and T. Y. Al-Naffouri, “Coexisting terahertz and RF finite wireless networks: Coverage and rate analysis,” *IEEE Trans. on Wireless Commun.*, 2022.
- [10] K. Dovelos, S. D. Assimonis, H. Q. Ngo, B. Bellalta, and M. Matthaiou, “Intelligent reflecting surfaces at terahertz bands: Channel modeling and analysis,” in *2021 IEEE International Conference on Communications Workshops (ICC Workshops)*. IEEE, 2021, pp. 1–6.